

Scissors Mode of Dipolar Quantum Droplets of Dysprosium Atoms

Igor Ferrier-Barbut,^{1,*} Matthias Wenzel,¹ Fabian Böttcher,¹ Tim Langen,¹
Mathieu Isoard,^{2,†} Sandro Stringari,² and Tilman Pfau¹

¹*Physikalisches Institut and Center for Integrated Quantum Science and Technology IQST, Universität Stuttgart, Pfaffenwaldring 57, 70550 Stuttgart, Germany*

²*INO-CNR BEC Center and Dipartimento di Fisica, Università di Trento, 38123 Povo, Italy*



(Received 19 December 2017; published 18 April 2018)

We report on the observation of the scissors mode of a single dipolar quantum droplet. The existence of this mode is due to the breaking of the rotational symmetry by the dipole-dipole interaction, which is fixed along an external homogeneous magnetic field. By modulating the orientation of this magnetic field, we introduce a new spectroscopic technique for studying dipolar quantum droplets. This provides a precise probe for interactions in the system, allowing us to extract a background scattering length for ¹⁶⁴Dy of 69(4)*a*₀. Our results establish an analogy between quantum droplets and atomic nuclei, where the existence of the scissors mode is also only due to internal interactions. They further open the possibility to explore physics beyond the available theoretical models for strongly dipolar quantum gases.

DOI: 10.1103/PhysRevLett.120.160402

The recent observation of quantum droplets in dipolar Bose-Einstein condensates (dBEC) [1–3] and in BEC mixtures [4–6] opens the opportunity to bridge the gap between dense quantum liquids, such as atomic nuclei and helium, and very dilute ultracold atomic samples. This link was reinforced by the observation of the self-bound character of quantum droplets [5–7]. Prior to this, several phenomena shared by dense quantum liquids and dilute superfluids were observed. In particular, the so-called scissors mode first observed in nuclei [8–10] was later predicted and observed in Bose-Einstein condensates in anisotropic external potentials [11,12]. In nuclei, this mode corresponds to the out-of-phase rotation of the neutrons and protons, and in BECs it is an angular oscillation around the anisotropy axis [13]. Its existence is a marker of the breaking of a rotational symmetry. A stark difference, however, between BECs and nuclei is that in the latter, the scissors mode arises only due to internal interactions. In contact-interacting BECs, this mode exists only in an anisotropic external potential; it vanishes in cylindrically symmetric traps.

Quantum droplets are liquidlike objects, bound by a mean-field attraction and stabilized by beyond mean-field effects [2,4]. Their collective modes are a revealing probe for their internal properties [3,14,15]. The scissors mode was theoretically explored in the context of dBEC in Ref. [16]. Here, we demonstrate that the anisotropy of the dipole-dipole interaction (DDI), set by the external homogeneous magnetic field, leads to a well-defined scissors mode in dipolar quantum droplets even in cylindrically symmetric trapping geometries. We parametrically excite this mode, and the high frequencies observed reveal the very strong intrinsic anisotropy of dipolar quantum droplets. In addition, it is known that this mode is well

defined only for low excitation amplitude, while it is nonlinearly coupled to other low-frequency modes for large excitation angles [13]. We observe clear signatures of this nonlinear mode coupling and use such coupling to excite a low-frequency mode. Altogether, these measurements represent a strong test of internal interactions in the droplets; we thus extract the value of the *s*-wave background scattering length of ¹⁶⁴Dy with good precision. We put this in perspective with previous measurements, highlighting the two- and many-body physics at play in dipolar quantum droplets of dysprosium.

Theory.—The scissors mode, corresponding to an angular oscillation, is naturally excited by the *z* component of the angular momentum operator $\hat{L}_z = \sum_{k=1}^N (x_k p_k^y - y_k p_k^x)$. In the experiment, this corresponds to a rotation of the external magnetic field axis around \hat{z} . We consider here dipoles oriented along the *y* direction [see Fig. 1(a)], thereby breaking rotational invariance in the *xy* plane, even in the presence of a cylindrically symmetric trap. Employing linear response theory, one can derive a rigorous upper bound to the frequency of the scissors mode in the form [13]

$$\hbar\omega_{sc} = \sqrt{\frac{m_1}{m_{-1}}}, \quad (1)$$

where $m_1 = \hbar^2 \int d\omega \omega S_{L_z}(\omega)$ is the energy-weighted moment of the dynamical structure factor $S_{L_z}(\omega)$, relative to the angular momentum operator, while $m_{-1} = \int d\omega / \omega S_{L_z}(\omega)$ is the inverse energy-weighted moment. Both moments m_1 and m_{-1} encapsulate important physical information on the scissors mode. The m_1 moment can, in

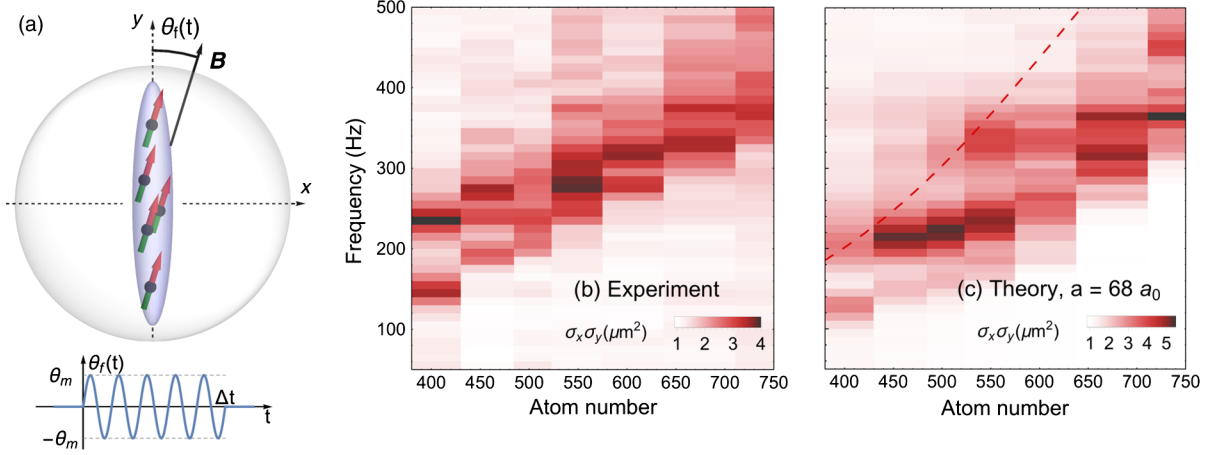


FIG. 1. (a) Experimental method: The quantum droplet is held in a cylindrically symmetric trap (around z); the orientation of the field is modulated around its mean value along y for $\Delta t = 20$ ms at variable frequency. The amplitude θ_m follows $\theta_m(f) = 12^\circ / \sqrt{f/100 \text{ Hz}}$. (b) Experimental response measured as a growth in the visible size of the droplet $\sigma_x \times \sigma_y$, as a function of atom number and modulation frequency. (c) The theory shows the same value extracted from solutions of the equations of motion within the Gaussian ansatz using the best-fit value of $a = 68a_0$. It takes into account the finite excitation time as well as departure from the linear response regime. The shot-to-shot fluctuations in atom number are simulated, and finite resolution is also implemented in the theory calculation of $\sigma_x \times \sigma_y$. Note the different scales for theory and experiments; the $\sim 20\%$ difference in droplet size could be due to imaging miscalibration. The dashed line shows the theoretical scissors mode frequency in linear response theory; see Ref. [17].

fact, be expressed in terms of a double commutator involving the Hamiltonian of the system as

$$m_1(\hat{L}_z) = \frac{1}{2} \langle [\hat{L}_z, [\hat{H}, \hat{L}_z]] \rangle \quad (2)$$

and can be regarded as an effective restoring force parameter for the scissors oscillation. Here $\langle \cdot \rangle$ is the average taken on the equilibrium configuration of the system. The nonvanishing of the commutator $[\hat{H}, \hat{L}_z]$ is the consequence of the breaking of rotational invariance. This can be due to the presence of an anisotropic trapping potential, and/or to the presence of the dipolar interaction. In the case we are interested in, of isotropic harmonic trapping ($\omega_x = \omega_y \equiv \omega_\perp$) (or in the absence of trapping), only the dipolar interaction contributes to the commutator, and the m_1 sum rule takes the useful form (see Supplemental Material [17])

$$m_1 = \frac{\hbar^2}{2} (\langle V_{\text{dd}}^x \rangle - \langle V_{\text{dd}}^y \rangle), \quad (3)$$

where $\langle V_{\text{dd}}^\alpha \rangle = \int d\mathbf{r} d\mathbf{r}' n(\mathbf{r}) V_{\text{dd}}^\alpha(\mathbf{r} - \mathbf{r}') n(\mathbf{r}')$, and $V_{\text{dd}}^\alpha(\mathbf{r}) = (\mu_0 \mu^2 / 4\pi r^3) [1 - 3(\alpha^2 / r^2)]$, $\alpha = x, y, z$. Equation (3) emphasizes the crucial role played by the dipolar interaction, which causes an asymmetry between the ground-state expectation values $\langle V_{\text{dd}}^x \rangle$ and $\langle V_{\text{dd}}^y \rangle$. For ^{164}Dy $\mu \approx 10\mu_B$, with μ_B the Bohr magneton, this defines the dipolar length $a_{\text{dd}} = (\mu_0 \mu^2 m / 12\pi \hbar^2)$, compared to the s -wave scattering length a via $\varepsilon_{\text{dd}} = a_{\text{dd}} / a$.

Differently from m_1 , the inverse energy-weighted moment m_{-1} cannot be written in terms of commutators,

but it can be usefully identified in terms of the moment of inertia Θ of the system. Actually, the moment m_{-1} corresponds, apart from a factor $1/2$, to the static response of the system to an angular momentum perturbation of the form $-\omega \hat{L}_z$. The moment of inertia, which provides the mass parameter of the scissors oscillation, is very sensitive to superfluidity, and for a Bose-Einstein condensate at zero temperature, is given by the expression [13]

$$\Theta = 2m_{-1} = m \frac{(\langle y^2 \rangle - \langle x^2 \rangle)^2}{\langle y^2 \rangle + \langle x^2 \rangle}, \quad (4)$$

which follows from the irrotationality constraint characterizing the superfluid velocity. For an axisymmetric configuration, the moment of inertia of a superfluid then identically vanishes.

All the average quantities characterizing the moments m_1 and m_{-1} can be evaluated using the Gaussian ansatz $\psi(\mathbf{r}) = (\sqrt{N} / \pi^{3/4} \bar{\sigma}^{3/2}) e^{-\sum_\alpha (r_\alpha^2 / 2\bar{\sigma}_\alpha^2)}$ for the order parameter relative to the ground state, with $\alpha \in \{x, y, z\}$ and $\bar{\sigma}^3 = \sigma_x \sigma_y \sigma_z$. The square radii, entering the expression for the moment of inertia, are given by $\langle r_i^2 \rangle = \sigma_i^2 / 2$. The values $\langle V_{\text{dd}}^x \rangle$ and $\langle V_{\text{dd}}^y \rangle$, entering the m_1 sum rule, can also be calculated using the Gaussian ansatz, and in the general case of anisotropic trapping we recover the results for dipolar BECs obtained in Ref. [16]. The expression for the resulting scissors mode frequency $\hbar\omega_{\text{sc}} = \sqrt{m_1 / m_{-1}}$ is reported as Eq. (S13) in Ref. [17]. It is worth noticing that the calculated equilibrium sizes σ_i , obtained through a variational procedure applied to the energy of the system, strongly depend on the scattering length a [14,20], which

gives an implicit dependence of the scissors frequency on a . We have checked that a time-dependent simulation, based on extended Gross-Pitaevskii (eGPE) theory, agrees in the linear limit with the sum rule value for the scissors frequency calculated using the Gaussian ansatz. The basic ingredients underlying the dynamics of the scissors mode are indeed well captured by the sum rule approach. Actually, our result takes into account both the breaking of rotational symmetry caused by the dipolar interaction [see Eq. (3)] and the superfluid expression (4) for the moment of inertia, which, however, does not differ significantly from the classical rigid value $m(\langle x^2 \rangle + \langle y^2 \rangle)$ due to the large anisotropy of the dipolar droplet characterizing the present experimental conditions. The sum rule approach provides a reliable estimate of the scissors frequency in the linear regime. Experiments, however, involve relatively large amplitudes of the oscillation, and for a systematic quantitative comparison it is useful to develop a time-dependent extension of the variational approach. It is based on the Lagrangian formalism, where the Gaussian ansatz is generalized to include a phase playing the role of a velocity potential, as already employed for dipolar BECs in Ref. [21] and in Ref. [14] for quantum droplets, now with an additional parameter accounting for the orientation θ of the droplet in the xy plane. The new calculation, which corresponds to solving the equations of motion for the four degrees of freedom $\sigma_{x,y,z}$ and θ , accounts for the excitation of the scissors mode as well as that of additional low-frequency modes of quadrupole and compression nature, which play an important role in the nonlinear limit, as we will discuss below.

Experiments.—We perform experiments on dipolar quantum droplets in an optical dipole trap, in which we obtain lifetimes of several hundreds of milliseconds. The trapping configuration was presented in Ref. [22]. Here the trap has fixed frequencies of $f_x = f_y = 40(1)$ Hz, $f_z = 950$ Hz (\hat{z} being along gravity), and is thus isotropic in the xy plane, as assumed by the theory presented above. The magnetic field is always oriented in this plane, initially along \hat{y} . In such geometry, quantum droplets can exist for smaller atom numbers than in free space and for very small atom numbers outside the range of our experiments; similarly to Ref. [23], they transform into solitons [24,25], which differ from quantum droplets by being stable even without beyond-mean-field corrections; see Ref. [17]. To extract their properties, we fit column-integrated images with a Gaussian distribution $\bar{n} = (N/\pi\sigma_x\sigma_y) \exp[-(x^2/\sigma_x^2) - (y^2/\sigma_y^2)]$. We obtain a typical size along \hat{y} of $\sigma_y \sim 1.5 \mu\text{m}$, while the extent along \hat{x} is smaller than our resolution [17]. We create single droplets containing a few hundred atoms. Their density being initially high, the atom number decays fast from $N \approx 750$ down to $N \approx 400$ via three-body losses. The systematic uncertainty on the number of condensed atoms within the droplet is $\delta N/N = 0.25$ [17]. The absolute value of the

magnetic field is fixed to be $B_0 = 800$ mG, far from any Feshbach resonance [26], so that the scattering length takes the low-field background value a_{bg} .

In the first set of experiments, we parametrically excite the scissors mode by adding an oscillating magnetic field along \hat{x} , exemplified in Fig. 1(a). The x field follows $B_x(t) = B_{x0} \sin(2\pi ft)$, with a variable frequency f and a maximum amplitude of $B_{x0} \leq 200$ mG. The angle of the field with respect to the y axis θ_f is then $\theta_f(t) \simeq B_x(t)/B_0 = \theta_m \sin(2\pi ft)$. The modulation time is $\Delta t = 20$ ms, chosen so that atom numbers variations are small, $\Delta N/N \leq 10\%$, during this time. Since Δt is kept fixed, to keep a constant pulse “energy” we decrease the modulation amplitude with a $1/\sqrt{f}$ scaling: $\theta_m(f) = \theta_0/\sqrt{f/100 \text{ Hz}}$. We first perform our experiments with $\theta_0 = 12^\circ$.

When the field direction is modulated, we observe a clear excitation of the scissors mode. We show in Ref. [17] that this is not due to the very small modulation of the absolute field ($[(\delta|B|)/B_0] \leq 4 \times 10^{-2}$). The excitation is seen as an increase in the observed size of the droplet: $\sigma_x \times \sigma_y$. Since the atom number varies with time, we can investigate the variation of the response with atom number. We observe a clear dependence, shown in Fig. 1(b). The maximum response frequency clearly increases with atom number. We note that several features are also visible in Fig. 1(b). In particular, a splitting into two lines is observable at low atom numbers. These characteristics signal that the observed response contains more than a simple parametric excitation of the scissors mode in the linear response regime. The rather large anisotropy of dipolar quantum droplets even in symmetric traps leads to a well-defined scissors mode. However, as we impose values of the excitation angle close to the deformation $(\sigma_y^2 - \sigma_x^2)/(\sigma_x^2 + \sigma_y^2)$ of the atomic cloud, we expect to approach the regime where the scissors mode is not well defined as it couples to other low-lying modes [11].

To confirm that the line splitting for the lowest atom numbers is due to hybridization of the scissors mode, we perform experiments at a fixed atom number $N = 390(100)$, but for varying amplitude. This is represented in Fig. 2(b)—for low amplitude we obtain a much lower response, requiring much more data averaging to reach a sufficient signal-to-noise ratio. But we do observe that only one peak appears at lower amplitude, confirming that departure from the linear regime occurs for the amplitudes used in Fig. 1(b). In order to capture these effects, which come from a coupling between the different lowest-lying modes of the system, we compare the experimental results with the predictions of the variational time-dependent model introduced in the *Theory* section of this Letter and discussed in details in Ref. [17]. With this theoretical approach, we can implement the exact experimental field modulation and reproduce very well the line splitting as seen in Fig. 2(a). In addition, we can also obtain a good agreement between theory and experiments for the

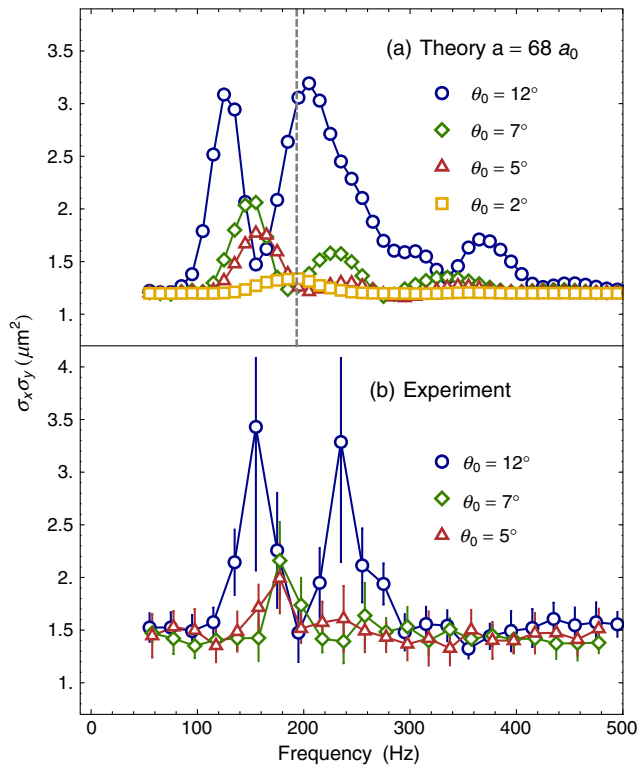


FIG. 2. Variation of the response with the angle modulation amplitude. Data and theory in Fig. 1 correspond to $\theta_0 = 12^\circ$. (a) Theory: We take $a = 68a_0$, as it gives the best fit over the whole range of atom numbers in Fig. 1; this explains the slight horizontal disagreement with experiment. For increasing excitation amplitude, the response increases, and a line splitting is observed due to departure from the linear response regime. The dashed line shows the linear response prediction. (b) Experiment, with atom number 390(100): The same increase in response and line splitting is observed. We surmise that the small peaks at high frequency absent in the experiment are due to the simplifying assumptions of our model.

range of atom numbers probed in Fig 1(b), with the scattering length as a single adjustable parameter. The result is shown in Fig. 1(c). In this plot, the scissors mode frequency is shown as a dashed line, showing that the departure from linear response causes a significant shift of the signal. Finally, this allows us to conclude on the scattering length for which our observations at different atom numbers and $\theta_0 = 12^\circ$ are best reproduced: $a = 68(5)a_0$, where the main contribution to the error is coming from the systematic uncertainty in the atom number [17]. When on the other hand we use only the low-amplitude data $\theta_0 = 5^\circ$ at $N = 390$ shown in Fig. 2, we obtain $a = 67(6)a_0$, in agreement.

The nonlinear coupling between the scissors and other low-lying modes provides us with a new tool to excite the latter. In the last part of this Letter, we use this to study the properties of the lowest mode. The mode coupling arises at large angles between the field and the droplet. To probe this regime, we perform a 90° rotation of the field at constant

$B_0 = 800$ mG in a time $t \simeq 3$ ms. Systematic imaging errors prevent the direct observation of angle oscillations. Nevertheless, we observe that the droplet quickly rotates by 90° . Via this field orientation quench, we obtain clear evidence for the excitation of a collective mode, seen as a time oscillation of the droplet length. These oscillations are strongly damped, and we are able to observe them up to times of about 20 ms [17]. We infer that these oscillations correspond to an excitation of the lowest-frequency collective mode of the system, observed in Ref. [3]. It consists essentially of a compression of the long axis of the droplet. Performing simulations of the equations of motion, we find that nonlinearities must be taken into account. We therefore compare our experiments to numerical solutions of the equations of motion as above, applying our exact experimental field sequence.

We vary the z trapping frequency f_z and record the variation in the trapping frequency of oscillation over the first 10 to 20 ms. The experimental data are shown in Fig. 3, where we observe very little shift. We compare our measurements to theory and obtain relatively good agreement, though the increase in frequency predicted by theory is not clear in the experimental data. The best agreement is obtained for $a = 70.5(6.0)a_0$. This value is compatible with the scattering length extracted from the scissors mode parametric excitation.

The scattering length values extracted here allow us to conclude on the interactions present in Dy ultracold samples at $B = 800$ mG so that $a = a_{\text{bg}}$. The error-weighted mean experimental value from the two measurements is $a_{\text{bg}} = 69(4)a_0$. Values obtained in noncondensed samples [27–29] are consistently higher than that reported in quantum droplets [7], though with large error bars. This

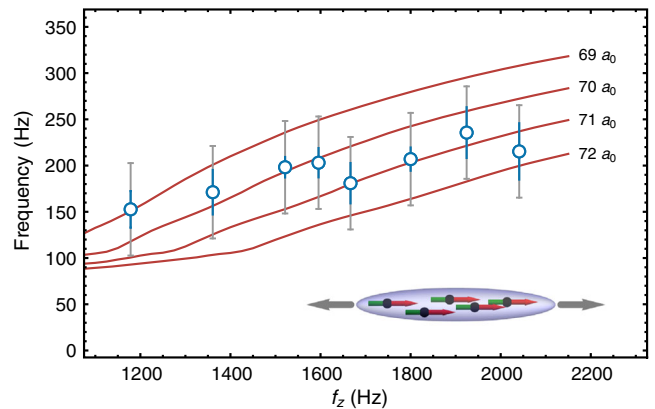


FIG. 3. Long axis oscillation frequency following a 90° field angle quench. Experiments are performed with an atom number of 690 (150). The error bar in blue shows the result of a squared sum of the fit standard error and the fitted decay time. The grey error bars show a 100 Hz interval corresponding to the short observation time. The red lines are theory calculations using the equations of motion for different scattering lengths (indicated on the figure).

might stem from the effect theoretically predicted in Ref. [30] of an effective dipole-dipole interaction dependent on collisional energy. Systematic measurements, for instance using the lattice method of Ref. [3], could shed further light into the two-body interactions, which can no longer be described by a simple addition of the DDI potential and the effective contact interaction potential [31,32]. An interesting direction to further explore is to try to compare precise measurements of collective mode frequencies on one side and critical atom number in self-bound droplets on the other side. Indeed, these precise spectroscopic probes should hold a signature of departure from the eGPE description of the system, a breakdown of the local density approximation should be expected, and the critical atom number might depend on details of the potential beyond the s -wave scattering length, as was shown for Bose mixtures in Ref. [33]. Quantum Monte Carlo works like Refs. [34–36] will need to include two-body interaction potentials faithful to the real Dy-Dy potential.

In conclusion, our work sheds new light on dipolar quantum droplets, demonstrating a macroscopic collective mode shared with atomic nuclei. In both systems, this mode is due to internal interactions, though for the present case of dipolar quantum droplets, the rotational symmetry is broken by the external homogeneous magnetic field, while it is spontaneously broken in nuclei. We showed that the method developed here is a powerful probe for interactions in dipolar quantum droplets, and its systematic application should lead to the observation of physics beyond the current theoretical level.

The Stuttgart group would like to acknowledge discussions with John Bohn. S. S. thanks Russell Bisset for useful comments and acknowledges funding from the Provincia Autonoma di Trento and the QUIC grant of the European Horizon2020 FET program. This work is supported by the German Research Foundation (DFG) within FOR2247. I. F. B. and T. L. acknowledge support from the EU within Horizon2020 Marie Skłodowska Curie IF (Grants No. 703419 DipInQuantum and No. 746525 coolDips, respectively). T. L. acknowledges support from the Alexander von Humboldt Foundation through a Feodor Lynen Fellowship.

*i.ferrier-barbut@physik.uni-stuttgart.de

†Present address: LPTMS, CNRS, Univ. Paris-Sud, Université Paris-Saclay, 91405 Orsay, France.

- [1] H. Kadau, M. Schmitt, M. Wenzel, C. Wink, T. Maier, I. Ferrier-Barbut, and T. Pfau, Observing the Rosensweig instability of a quantum ferrofluid, *Nature (London)* **530**, 194 (2016).
- [2] I. Ferrier-Barbut, H. Kadau, M. Schmitt, M. Wenzel, and T. Pfau, Observation of Quantum Droplets in a Strongly Dipolar Bose Gas, *Phys. Rev. Lett.* **116**, 215301 (2016).
- [3] L. Chomaz, S. Baier, D. Petter, M. J. Mark, F. Wächtler, L. Santos, and F. Ferlaino, Quantum-Fluctuation-Driven Crossover from a Dilute Bose-Einstein Condensate to a Macrodroplet in a Dipolar Quantum Fluid, *Phys. Rev. X* **6**, 041039 (2016).
- [4] D. S. Petrov, Quantum Mechanical Stabilization of a Collapsing Bose-Bose Mixture, *Phys. Rev. Lett.* **115**, 155302 (2015).
- [5] C. R. Cabrera, L. Tanzi, J. Sanz, B. Naylor, P. Thomas, P. Cheiney, and L. Tarruell, Quantum liquid droplets in a mixture of Bose-Einstein condensates, *Science* **359**, 301 (2018).
- [6] G. Semeghini, G. Ferioli, L. Masi, C. Mazzinghi, L. Wolswijk, F. Minardi, M. Modugno, G. Modugno, M. Inguscio, and M. Fattori, Self-bound quantum droplets in atomic mixtures, [arXiv:1710.10890](https://arxiv.org/abs/1710.10890).
- [7] M. Schmitt, M. Wenzel, F. Böttcher, I. Ferrier-Barbut, and T. Pfau, Self-bound droplets of a dilute magnetic quantum liquid, *Nature (London)* **539**, 259 (2016).
- [8] N. Lo Iudice and F. Palumbo, New Isovector Collective Modes in Deformed Nuclei, *Phys. Rev. Lett.* **41**, 1532 (1978).
- [9] E. Lipparini and S. Stringari, Isovector M1 rotational states in deformed nuclei, *Phys. Lett.* **130B**, 139 (1983).
- [10] J. Enders, H. Kaiser, P. von Neumann-Cosel, C. Rangacharyulu, and A. Richter, Comprehensive analysis of the scissors mode in heavy even-even nuclei, *Phys. Rev. C* **59**, R1851 (1999).
- [11] D. Guéry-Odelin and S. Stringari, Scissors Mode and Superfluidity of a Trapped Bose-Einstein Condensed Gas, *Phys. Rev. Lett.* **83**, 4452 (1999).
- [12] O. M. Maragò, S. A. Hopkins, J. Arlt, E. Hodby, G. Hechenblaikner, and C. J. Foot, Observation of the Scissors Mode and Evidence for Superfluidity of a Trapped Bose-Einstein Condensed Gas, *Phys. Rev. Lett.* **84**, 2056 (2000).
- [13] L. Pitaevskii and S. Stringari, *Bose-Einstein Condensation and Superfluidity*, Vol. 164 (Oxford University Press, New York, 2016).
- [14] F. Wächtler and L. Santos, Ground-state properties and elementary excitations of quantum droplets in dipolar Bose-Einstein condensates, *Phys. Rev. A* **94**, 043618 (2016).
- [15] D. Baillie, R. M. Wilson, and P. B. Blakie, Collective Excitations of Self-Bound Droplets of a Dipolar Quantum Fluid, *Phys. Rev. Lett.* **119**, 255302 (2017).
- [16] R. M. W. van Bijnen, N. G. Parker, S. J. J. M. F. Kokkelmans, A. M. Martin, and D. H. J. O'Dell, Collective excitation frequencies and stationary states of trapped dipolar Bose-Einstein condensates in the Thomas-Fermi regime, *Phys. Rev. A* **82**, 033612 (2010).
- [17] See Supplemental Material at <http://link.aps.org/supplemental/10.1103/PhysRevLett.120.160402> for the theoretical derivation of the scissors mode frequency as well as details of the experimental procedure and data analysis, which includes Refs. [18,19].
- [18] K. Glaum and A. Pelster, Bose-Einstein condensation temperature of dipolar gas in anisotropic harmonic trap, *Phys. Rev. A* **76**, 023604 (2007).
- [19] S. Giovanazzi, P. Pedri, L. Santos, A. Griesmaier, M. Fattori, T. Koch, J. Stuhler, and T. Pfau, Expansion dynamics of a dipolar Bose-Einstein condensate, *Phys. Rev. A* **74**, 013621 (2006).
- [20] R. N. Bisset, R. M. Wilson, D. Baillie, and P. B. Blakie, Ground-state phase diagram of a dipolar condensate with quantum fluctuations, *Phys. Rev. A* **94**, 033619 (2016).

- [21] S. Yi and L. You, Trapped condensates of atoms with dipole interactions, *Phys. Rev. A* **63**, 053607 (2001).
- [22] M. Wenzel, F. Böttcher, T. Langen, I. Ferrier-Barbut, and T. Pfau, Striped states in a many-body system of tilted dipoles, *Phys. Rev. A* **96**, 053630 (2017).
- [23] P. Cheiney, C. R. Cabrera, J. Sanz, B. Naylor, L. Tanzi, and L. Tarruell, Bright Soliton to Quantum Droplet Transition in a Mixture of Bose-Einstein Condensates, *Phys. Rev. Lett.* **120**, 135301 (2018).
- [24] I. Tikhonenkov, B. A. Malomed, and A. Vardi, Anisotropic Solitons in Dipolar Bose-Einstein Condensates, *Phys. Rev. Lett.* **100**, 090406 (2008).
- [25] P. Köberle, D. Zajec, G. Wunner, and B. A. Malomed, Creating two-dimensional bright solitons in dipolar Bose-Einstein condensates, *Phys. Rev. A* **85**, 023630 (2012).
- [26] K. Baumann, N. Q. Burdick, M. Lu, and B. L. Lev, Observation of low-field Fano-Feshbach resonances in ultracold gases of dysprosium, *Phys. Rev. A* **89**, 020701 (2014).
- [27] Y. Tang, A. Sykes, N. Q. Burdick, J. L. Bohn, and B. L. Lev, s -wave scattering lengths of the strongly dipolar bosons ^{162}Dy and ^{164}Dy , *Phys. Rev. A* **92**, 022703 (2015).
- [28] T. Maier, I. Ferrier-Barbut, H. Kadau, M. Schmitt, M. Wenzel, C. Wink, T. Pfau, K. Jachymski, and P. S. Julienne, Broad universal Feshbach resonances in the chaotic spectrum of dysprosium atoms, *Phys. Rev. A* **92**, 060702 (2015).
- [29] Y. Tang, A. G. Sykes, N. Q. Burdick, J. M. DiSciaccia, D. S. Petrov, and B. L. Lev, Anisotropic Expansion of a Thermal Dipolar Bose Gas, *Phys. Rev. Lett.* **117**, 155301 (2016).
- [30] R. Oldziejewski and K. Jachymski, Properties of strongly dipolar Bose gases beyond the Born approximation *Phys. Rev. A* **94**, 063638 (2016); Erratum, **95**, 049901 (2017).
- [31] D. C. E. Bortolotti, S. Ronen, J. L. Bohn, and D. Blume, Scattering Length Instability in Dipolar Bose-Einstein Condensates, *Phys. Rev. Lett.* **97**, 160402 (2006).
- [32] R. Oldziejewski and K. Jachymski, Properties of strongly dipolar Bose gases beyond the Born approximation, *Phys. Rev. A* **94**, 063638 (2016).
- [33] V. Cikojević, K. Dželalija, P. Stipanović, L. Vranješ Markić, and J. Boronat, Ultradilute quantum liquid drops, *Phys. Rev. B* **97**, 140502(R) (2018).
- [34] H. Saito, Path-integral Monte Carlo study on a droplet of a dipolar Bose-Einstein condensate stabilized by quantum fluctuation, *J. Phys. Soc. Jpn.* **85**, 053001 (2016).
- [35] A. Macia, J. Sánchez-Baena, J. Boronat, and F. Mazzanti, Droplets of Trapped Quantum Dipolar Bosons, *Phys. Rev. Lett.* **117**, 205301 (2016).
- [36] F. Cinti, A. Cappellaro, L. Salasnich, and T. Macrì, Superfluid Filaments of Dipolar Bosons in Free Space, *Phys. Rev. Lett.* **119**, 215302 (2017).